Proceedings Paper:

Hill, T.L., Cammarano, A., Neild, S.A. et al. (1 more author) (2014) An analytical method for the optimisation of weakly nonlinear systems. In: Proceedings of EURODYN 2014. EURODYN 2014 9th International Conference on Structural Dynamics, 30 June – 2 July 2014, Porto, Portugal. , 1981 - 1988. ISBN 978-972-752-165-4

Proceedings of the 9th International Conference on Structural Dynamics, EURODYN 2014
Porto, Portugal, 30 June - 2 July 2014
A. Cunha, E. Caetano, P. Ribeiro, G. Müller (eds.)
ISSN: 2311-9020; ISBN: 978-972-752-165-4

An analytical method for the optimisation of weakly nonlinear systems

T.L. Hill[1], A. Cammarano[1], S.A. Neild[1], D.J. Wagg[2]
[1]Department of Mechanical Engineering, University of Bristol, Bristol, BS8 1TR, UK
[2]Department of Mechanical Engineering, University of Sheffield, Sheffield, S1 3JD, UK
email: tom.hill@bristol.ac.uk, andrea.cammarano@bristol.ac.uk, simon.neild@bristol.ac.uk, david.wagg@sheffield.ac.uk

ABSTRACT: In this paper we discuss how backbone curves can be used to guide the design and optimisation of weakly nonlinear systems with multiple degrees-of-freedom. After decomposing the system using the modes of the equivalent linear system (the linear modes), we show how the backbone curves of the unforced, undamped equivalent system can be calculated. These consist of pure responses in each of the linear modes and, in certain parameter regimes, responses which are a combination of two or more linear modes - a feature which can be linked to internal resonance. Using an example system we will investigate how these backbone curves can be used to describe particular characteristics of the response. An energy balancing technique is also employed to relate the backbone curves to the response of the forced and damped system, and anticipate the conditions for which a particular characteristic will be seen. Finally, we discuss how the analytical nature of these techniques enables us to precisely design and optimise characteristics of such systems and how this can be expanded to systems with a greater number of degrees-of-freedom.

KEY WORDS: Nonlinear dynamics; Backbone curves; Second-order normal forms; Energy balancing.

1 INTRODUCTION

A major challenge for structural engineers is dealing with nonlinear behaviours. The demand for lighter and more efficient structures brings with it a requirement that structures operate beyond the limits where linearity may be assumed. To design structures with nonlinear characteristics, engineers must be able to predict their response and understand how these characteristics may be exploited and designed into structures. One existing approach to modelling nonlinear dynamic behaviour is using numerical continuation programmes, such as AUTO-07p [1], which provides an accurate solution to the differential equations describing the system. However this provides little insight into the relationships between the characteristics of the system and the response and becomes increasingly complex and involved for large systems, making it unsuitable for many practical applications.

Analytical and semi-analytical techniques provide greater insight into the relationships within systems and offer greater scalability. Nonlinear normal modes, see [2] and [3], are one such technique and can provide insight into the behaviour of nonlinear structures, and their resonant interactions. Approaches such as perturbation and harmonic balance techniques [4] provide good, analytical approximations to weakly nonlinear systems, although they also become increasingly complex with scale and thus ill-suited for large systems. Methods for automating these techniques do allow for an expansion in the complexity of the systems they are used to model, see for example [5] and [6].

In this work an approach based on the second-order normal form technique is presented. This is used to not only describe the response of the nonlinear system, but also to derive expressions relating the behaviours in the response to the physical parameters describing the system. This allows for the development of expressions that may be used for the optimisation of systems operating in the nonlinear regime. The backbone curves, describing the response of the unforced, undamped equivalent system, provide a simple description of the system and hence are used in this work as a starting point. They also highlight the interactions that may occur within the system whilst relating to the behaviour of the response when the system is forced and damped.

Section 2 gives a step-by-step description of the application of the second-order normal form technique when used to calculate the backbone curves for systems with multiple-degrees-of-freedom (MDOF), and the motivation for each transform is explained. In Section 3, this approach is demonstrated for a two-mass oscillator with a nonlinear spring, where the nonlinear component is described by a single parameter. This results in a set of expressions describing the backbone curves of the system, which are then used to derive expressions for the relationship between particular aspects of the response of the system and the nonlinear parameter. Section 4 introduces an energy-based technique which allows the relationship between the backbone curves and the forced response to be specified. These descriptions of the dynamics of the system are then combined in Section 5, where the system is optimised. Conclusions are then drawn in Section 6.

2 THE SECOND-ORDER NORMAL FORM TECHNIQUE

The second-order normal form technique allows the behaviour of weakly nonlinear systems to be described analytically; where here, analytical solutions are also assumed to be approximate. This enables the design and optimisation of the response of such systems based on their physical characteristics, making it a valuable tool for the analysis considered here. This technique is applied directly to systems described in the second-order differential form; a more natural formulation of engineering problems. This gives advantages over the first-order (state-space based) approach [7] with regard to both the ease of formulation, and improved accuracy [9]. The approach also has advantages over numerical techniques, such as continuation approaches (for example AUTO-07p, [1]) and nonlinear normal modes (where an analytical solution can only be found in certain circumstances), see for example [2] and [3]. The second-order normal form technique is limited to smooth, lightly damped, weakly-nonlinear systems – i.e. systems operating in regimes where the nonlinear (and damping) terms are small in comparison to the undamped linear terms.

A number of works describe the technique, for example [8], [9] and [10], for a broad range of systems. For completeness, a description is given of the application of the technique to the class of system considered here (i.e. for computation of the backbone curves of MDOF systems).

2.1 PROBLEM FORMULATION

Consider a forced and damped nonlinear system with N degrees-of-freedom, whose equation of motion can be written

$$\mathbf{M}\ddot{\mathbf{x}} + \mathbf{C}\dot{\mathbf{x}} + \mathbf{K}\mathbf{x} + \boldsymbol{\Gamma}_x(\mathbf{x}) = \mathbf{P}_x \cos(\Omega t), \tag{1}$$

where: $\mathbf{x}$ is an $N \times 1$ vector of displacements; $\mathbf{M}$, $\mathbf{C}$ and $\mathbf{K}$ are $N \times N$ mass, damping and stiffness matrices respectively; $\boldsymbol{\Gamma}_x(\mathbf{x})$ is an $N \times 1$ vector of nonlinear terms; and $\mathbf{P}_x$ is an $N \times 1$ vector of forcing amplitudes. Note that $\boldsymbol{\Gamma}_x(\mathbf{x})$ is a function of displacement only – i.e. the system has no nonlinear damping or forcing. To find the backbone curves of this system, we require the underlying conservative system, which may be written

$$\mathbf{M}\ddot{\mathbf{x}} + \mathbf{K}\mathbf{x} + \boldsymbol{\Gamma}_x(\mathbf{x}) = 0. \tag{2}$$

2.2 LINEAR MODAL TRANSFORM ($\mathbf{x} \to \mathbf{q}$)

The system described by Eq. (2) can now be projected onto the underlying linear system by applying the linear modal transform $\mathbf{x} = \boldsymbol{\Phi}\mathbf{q}$. Here, $\boldsymbol{\Phi}$ is an $N \times N$ matrix where the n^{th} column describes the modeshape of the n^{th} linear mode. These can be found as the eigenvectors of $\mathbf{M}^{-1}\mathbf{K}$, where the corresponding eigenvalues are ω_{nn}^2 (the square of the natural frequency of the n^{th} linear mode). This transform leads to the modal dynamic equation

$$\ddot{\mathbf{q}} + \boldsymbol{\Lambda}\mathbf{q} + \mathbf{N}_q(\mathbf{q}) = 0, \tag{3}$$

where $\boldsymbol{\Lambda}$ is an $N \times N$ diagonal matrix where n^{th} leading diagonal element is ω_{nn}^2.

In its typical formulation, the next step of the second-order normal form technique is the forcing transform, which removes all forcing terms that are not close to the response frequencies of the linear modes. As this formulation only concerns unforced systems, this step is omitted.

2.3 NONLINEAR NEAR-IDENTITY TRANSFORM ($\mathbf{q} \to \mathbf{u}$)

The final step in the technique is the nonlinear near-identity transform. Here, the transform $\mathbf{q} = \mathbf{u} + \mathbf{h}(\mathbf{u})$ is applied to Eq. (3), leading to

$$\ddot{\mathbf{u}} + \boldsymbol{\Lambda}\mathbf{u} + \mathbf{N}_u(\mathbf{u}) = 0. \tag{4}$$

Here, $\mathbf{u}$ is an $N \times 1$ vector describing the fundamental response of $\mathbf{q}$, and $\mathbf{h}$ is an $N \times 1$ vector containing all of the harmonic contents of $\mathbf{q}$. By defining $\mathbf{h}$ as a function of $\mathbf{u}$ (i.e. treating the harmonic contents of the response as a function of the fundamental response) we may determine the total response of $\mathbf{q}$ from a solution for $\mathbf{u}$. In this transform we require $\mathbf{h}$ to be small, such that the transform is near-identity. Using ε, a bookkeeping parameter denoting *smallness*, we may write $\mathbf{h}$ as $\mathbf{h} = \varepsilon\hat{\mathbf{h}}$, indicating the smallness of $\mathbf{h}$. By applying a power series expansion in ε, we may write $\mathbf{h}$ as $\mathbf{h} = \varepsilon\hat{\mathbf{h}}_1 + \varepsilon^2\hat{\mathbf{h}}_2 + \varepsilon^3\hat{\mathbf{h}}_3 + ...$, from which we can approximate $\mathbf{h} \approx \mathbf{h}_1$. As we are assuming the nonlinear terms to be small (i.e. $\mathbf{N}_q = \varepsilon\hat{\mathbf{N}}_q$ and $\mathbf{N}_u = \varepsilon\hat{\mathbf{N}}_u$), we can also make the approximations $\mathbf{N}_q \approx \mathbf{n}_{q1}$ and $\mathbf{N}_u \approx \mathbf{n}_{u1}$.

We may now find a solution for Eq. (4) using the substitution for the n^{th} element of $\mathbf{u}$

$$\begin{aligned} u_n &= U_n \cos(\omega_{rn} t - \phi_n), \\ &= u_{np} + u_{nm} = \frac{U_n}{2}\left(\mathrm{e}^{+\mathrm{j}(\omega_{rn} t - \phi_n)} + \mathrm{e}^{-\mathrm{j}(\omega_{rn} t - \phi_n)}\right), \end{aligned} \tag{5}$$

where U_n, ω_{rn} and ϕ_n are the amplitude, frequency and phase of the response u_n. The subscripts p and m denote the positive and negative powers of the exponentials respectively. Note that the response frequency, ω_{rn}, of u_n is distinct from the linear natural frequency, ω_{nn}, of q_n.

We now make the approximation $\mathbf{q} = \mathbf{u} = \mathbf{u}_p + \mathbf{u}_m$, true to first-order accuracy as $\mathbf{h}$ is small, an substitute this into Eq. (3). From this we can define the $L \times 1$ vector $\mathbf{u}^*(\mathbf{u}_p, \mathbf{u}_m)$, containing the L unique combinations of $\mathbf{u}_p$ and $\mathbf{u}_m$. We may also define the $N \times L$ matrices $[n_q]$, $[n_u]$ and $[h]$ containing all coefficients of the terms in $\mathbf{u}^*$, such that

$$\mathbf{n}_{q1} = [n_q]\mathbf{u}^*, \quad \mathbf{n}_{u1} = [n_u]\mathbf{u}^*, \quad \mathbf{h}_1 = [h]\mathbf{u}^*. \tag{6}$$

The ℓ^{th} element of $\mathbf{u}^*$ can be written

$$u_\ell^* = \prod_{n=1}^{N} \{u_{np}^{s_{n\ell p}} u_{nm}^{s_{n\ell m}}\}. \tag{7}$$

From this we can determine which terms resonate at the response frequencies ω_{rn}. These terms will contribute to the fundamental response, $\mathbf{u}$, whilst the non-resonant terms will be stored in the vector of harmonic components $\mathbf{h}$. The resonant terms can be determined as the elements in the $N \times L$ matrix $\boldsymbol{\beta}$ with a value of zero. Element $(n,\ \ell)$ of $\boldsymbol{\beta}$ is calculated as

$$\beta_{n\ell} = \left[\sum_{k=1}^{N} \left\{(s_{\ell kp} - s_{\ell km})\omega_{rk}\right\}\right]^2 - \omega_{rn}^2, \tag{8}$$

where $s_{\ell kp}$ and $s_{\ell km}$ are defined in Eq. (7). Now, the elements in $[n_u]$ and $[h]$ corresponding to those in $\boldsymbol{\beta}$ can be calculated as

$$\beta_{n\ell} = 0 \quad \to \quad n_{u,n\ell} = n_{q,n\ell} \quad \& \quad h_{n\ell} = 0, \tag{9a}$$

$$\beta_{n\ell} \neq 0 \quad \to \quad n_{u,n\ell} = 0 \quad \& \quad h_{n\ell} = n_{q,n\ell}/\beta_{n\ell}. \tag{9b}$$

From Eq. (6) we can now use $[n_u]$ and $\mathbf{u}^*$ to find $\mathbf{n}_{u1}$, and hence $\mathbf{N}_u$. Substituting this into Eq. (4) we can then calculate $\mathbf{u}$. To find the harmonic content, we can substitute the calculated values of $\mathbf{u}$ into the expression for $\mathbf{h}$ (found using Eqs. (6) and (9)). The total modal response can then be found using $\mathbf{q} = \mathbf{u} + \mathbf{h}$, and the response in the physical coordinates is calculated by $\mathbf{x} = \boldsymbol{\Phi}\mathbf{q}$.

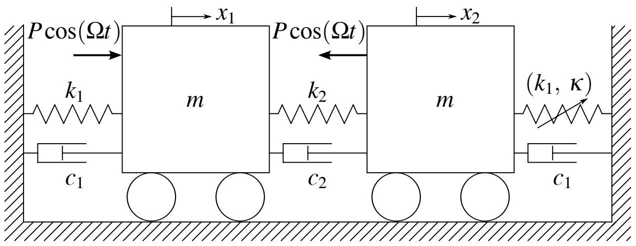

Figure 1. Schematic diagram of a two-degree-of-freedom oscillator. The underlying unforced, linear system is symmetric and a nonlinearity creates an asymmetry.

3 EXAMPLE: A TWO DEGREE-OF-FREEDOM SYSTEM

Figure 1 shows a forced, damped system with two degrees-of-freedom. The underlying linear, conservative system is symmetric, the damping is symmetric and linear, and the forcing is antisymmetric. The spring connecting the second mass to ground is nonlinear, creating an asymmetry in the system. This is a Duffing-type spring with the force-deflection relationship $F = k_1(\Delta x) + \kappa(\Delta x)^3$, where (Δx) is the displacement of the spring. The linear spring grounding the first mass has spring constant k_1, and the linear dampers connecting the masses to ground both have damping constants c_1. The linear spring and damper connecting the two masses have constants k_2 and c_2 respectively. A sinusoidal forcing, with amplitude P at frequency Ω, acts on both masses, but in anti-phase. This is equivalent to writing the forcing amplitudes acting on the first and second mass as $P_1 = P$ and $P_2 = -P$ respectively.

For the system considered, we use the parameter values

$$\begin{aligned} m &= 1, & k_1 &= 1, & k_2 &= 0.105, \\ P &= 0.005, & c_1 &= 0.005, & c_2 &= 0.005, \end{aligned} \tag{10}$$

whilst $\kappa > 0$ and may be varied. This system may be described in the form of Eq. (1) where

$$\mathbf{M} = \begin{bmatrix} 1 & 0 \\ 0 & 1 \end{bmatrix}, \quad \mathbf{C} = \begin{bmatrix} 0.01 & -0.005 \\ -0.005 & 0.01 \end{bmatrix},$$

$$\mathbf{K} = \begin{bmatrix} 1.105 & -0.105 \\ -0.105 & 1.105 \end{bmatrix}, \quad \boldsymbol{\Gamma}_x = \begin{pmatrix} 0 \\ \kappa x_2^3 \end{pmatrix}, \tag{11}$$

$$\mathbf{P}_x = \begin{pmatrix} 0.005 \\ -0.005 \end{pmatrix} \cos(\Omega t). \tag{12}$$

Finding the eigenvalues and eigenvectors of $\mathbf{M}^{-1}\mathbf{K}$, results in

$$\boldsymbol{\Lambda} = \begin{bmatrix} 1 & 0 \\ 0 & 1.21 \end{bmatrix}, \quad \boldsymbol{\Phi} = \begin{bmatrix} 1 & 1 \\ 1 & -1 \end{bmatrix}. \tag{13}$$

Hence, the linear natural frequencies are $\omega_{n1} = 1$ and $\omega_{n2} = 1.1$. Now, performing the linear modal transform results in

$$\ddot{\mathbf{q}} + \boldsymbol{\Lambda}\mathbf{q} + \mathbf{N}_q = \mathbf{P}_q, \tag{14}$$

where:

$$\mathbf{N}_q = \begin{pmatrix} +1 \\ -1 \end{pmatrix} \frac{\kappa(q_1 - q_2)^3}{2m} + \begin{bmatrix} 0.005 & 0 \\ 0 & 0.015 \end{bmatrix} \dot{\mathbf{q}},$$

$$\mathbf{P}_q = \begin{pmatrix} 0 \\ 0.005 \end{pmatrix} \cos(\Omega t). \tag{15}$$

Here, the damping and forcing terms have been included for use in the energy balancing technique considered later. First, however, the backbone curves of this system are calculated, in order to identify the underlying behaviour. This is achieved by neglecting the forcing and damping terms, and substituting $q_n \approx u_n = u_{np} + u_{nm}$, such that

$$\mathbf{N}_q = \frac{\kappa(u_{1p} + u_{1m} - u_{2p} - u_{2m})^3}{2m} \begin{pmatrix} +1 \\ -1 \end{pmatrix}. \tag{16}$$

Expanding this and using $\mathbf{N}_q = [n_q]\mathbf{u}^*$ gives

$$[n_q]^T = \frac{\kappa}{2m} \begin{bmatrix} 1 & -1 \\ 3 & -3 \\ 3 & -3 \\ 1 & -1 \\ 3 & -3 \\ 6 & -6 \\ 3 & -3 \\ 3 & -3 \\ 6 & -6 \\ 3 & -3 \\ -3 & 3 \\ -3 & 3 \\ -6 & 6 \\ -6 & 6 \\ -3 & 3 \\ -3 & 3 \\ -1 & 1 \\ -3 & 3 \\ -3 & 3 \\ -1 & 1 \end{bmatrix}, \quad \mathbf{u}^* = \begin{pmatrix} u_{1p}^3 \\ u_{1p}^2 u_{1m} \\ u_{1p} u_{1m}^2 \\ u_{1m}^3 \\ u_{1p} u_{2p}^2 \\ u_{1p} u_{2p} u_{2m} \\ u_{1p} u_{2m}^2 \\ u_{1m} u_{2p}^2 \\ u_{1m} u_{2p} u_{2m} \\ u_{1m} u_{2m}^2 \\ u_{1p}^2 u_{2p} \\ u_{1p}^2 u_{2m} \\ u_{1p} u_{1m} u_{2p} \\ u_{1p} u_{1m} u_{2m} \\ u_{1m}^2 u_{2p} \\ u_{1m}^2 u_{2m} \\ u_{2p}^3 \\ u_{2p}^2 u_{2m} \\ u_{2p} u_{2m}^2 \\ u_{2m}^3 \end{pmatrix}. \tag{17}$$

As ω_{n1} and ω_{n2} are close, it is assumed that the two modes will respond at the same frequency, which we will denote at Ω (i.e. $\Omega = \omega_{r1} = \omega_{r2}$). From $\mathbf{u}^*$, and using Eq. (8), we calculate $\boldsymbol{\beta}$ as

$$\boldsymbol{\beta}^T = \Omega^2 \begin{bmatrix} 8 & 8 \\ 0 & 0 \\ 0 & 0 \\ 8 & 8 \\ 8 & 8 \\ 0 & 0 \\ 0 & 0 \\ 0 & 0 \\ 0 & 0 \\ 8 & 8 \\ 8 & 8 \\ 0 & 0 \\ 0 & 0 \\ 0 & 0 \\ 0 & 0 \\ 8 & 8 \\ 8 & 8 \\ 0 & 0 \\ 0 & 0 \\ 8 & 8 \end{bmatrix}.$$

The zero terms in $\boldsymbol{\beta}$ satisfy the condition given by Eq. (9a), which we use to find the matrix $[n_u]$, and using Eq. (6) the nonlinear components of the fundamental response are found to be

$$\mathbf{n}_{u1} = \frac{3\kappa}{2m}\begin{pmatrix} (2u_{2p}u_{2m}+u_{1p}u_{1m})u_1 + u_{1p}u_{2m}^2 + u_{1m}u_{2p}^2 \\ (2u_{1p}u_{1m}+u_{2p}u_{2m})u_2 + u_{1p}^2u_{2m} + u_{1m}^2u_{2p} \\ -(2u_{1p}u_{1m}+u_{2p}u_{2m})u_2 - u_{1p}^2u_{2m} - u_{1m}^2u_{2p} \\ -(2u_{2p}u_{2m}+u_{1p}u_{1m})u_1 - u_{1p}u_{2m}^2 - u_{1m}u_{2p}^2 \end{pmatrix}. \quad (18)$$

This may be written in the form

$$\mathbf{n}_{u1} = \tilde{\mathbf{n}}_{u1}\mathrm{e}^{+\mathrm{j}\Omega t} + \bar{\mathbf{n}}_{u1}\mathrm{e}^{-\mathrm{j}\Omega t}, \quad (19)$$

where $\tilde{\mathbf{n}}_{u1}$ and $\bar{\mathbf{n}}_{u1}$ are complex conjugates. Substituting the expansions of u_{np} and u_{nm}, given in Eq. (5), and using $\phi_d = \phi_1 - \phi_2$, the $\tilde{\mathbf{n}}_{u1}$ component may be written

$$\tilde{\mathbf{n}}_{u1} = \frac{3\kappa}{16m}\begin{pmatrix} \left[U_1^2 + \left(2+\mathrm{e}^{+\mathrm{j}2\phi_d}\right)U_2^2 - U_1^{-1}U_2^3\mathrm{e}^{+\mathrm{j}\phi_d} - \left(2\mathrm{e}^{+\mathrm{j}\phi_d}+\mathrm{e}^{-\mathrm{j}\phi_d}\right)U_1U_2\right]U_1\mathrm{e}^{-\mathrm{j}\phi_1} \\ \left[\left(2+\mathrm{e}^{-\mathrm{j}2\phi_d}\right)U_1^2 + U_2^2 - U_1^3U_2^{-1}\mathrm{e}^{-\mathrm{j}\phi_d} - \left(2\mathrm{e}^{-\mathrm{j}\phi_d}+\mathrm{e}^{+\mathrm{j}\phi_d}\right)U_1U_2\right]U_2\mathrm{e}^{-\mathrm{j}\phi_2} \end{pmatrix}. \quad (20)$$

Substituting this into Eq. (4), and using $\mathbf{N}_u \approx \mathbf{n}_{u1}$ and $\ddot{\mathbf{u}} = -\Omega^2\mathbf{u}$, we find that Eq. (4) may be separated into complex conjugate parts, akin to Eq. (19). Taking the conjugate part corresponding to $\mathrm{e}^{+\mathrm{j}\Omega t}$ gives

$$\frac{1}{2}\begin{pmatrix} \left(\omega_{n1}^2-\Omega^2\right)U_1\mathrm{e}^{-\mathrm{j}\phi_1} \\ \left(\omega_{n2}^2-\Omega^2\right)U_2\mathrm{e}^{-\mathrm{j}\phi_1} \end{pmatrix}\mathrm{e}^{+\mathrm{j}\Omega t} + \tilde{\mathbf{n}}_{u1}\mathrm{e}^{+\mathrm{j}\Omega t} = \begin{pmatrix} 0 \\ 0 \end{pmatrix}, \quad (21)$$

which can be rearranged to

$$\left\{\omega_{n1}^2 - \Omega^2 + \frac{3\kappa}{8m}\left[U_1^2 + \left(2+\mathrm{e}^{+\mathrm{j}2\phi_d}\right)U_2^2 - U_1^{-1}U_2^3\mathrm{e}^{+\mathrm{j}\phi_d} - \left(2\mathrm{e}^{+\mathrm{j}\phi_d}+\mathrm{e}^{-\mathrm{j}\phi_d}\right)U_1U_2\right]\right\}U_1\mathrm{e}^{-\mathrm{j}\phi_1} = 0, \quad (22a)$$

$$\left\{\omega_{n2}^2 - \Omega^2 + \frac{3\kappa}{8m}\left[\left(2+\mathrm{e}^{-\mathrm{j}2\phi_d}\right)U_1^2 + U_2^2 - U_1^3U_2^{-1}\mathrm{e}^{-\mathrm{j}\phi_d} - \left(2\mathrm{e}^{-\mathrm{j}\phi_d}+\mathrm{e}^{+\mathrm{j}\phi_d}\right)U_1U_2\right]\right\}U_2\mathrm{e}^{-\mathrm{j}\phi_2} = 0. \quad (22b)$$

Assuming $U_1 \neq 0$ and $U_2 \neq 0$ this can be written

$$\omega_{d1} + \frac{3\kappa}{8m}\left[U_1^2 + \left(2+\mathrm{e}^{+\mathrm{j}2\phi_d}\right)U_2^2 - U_1^{-1}U_2^3\mathrm{e}^{+\mathrm{j}\phi_d} - \left(2\mathrm{e}^{+\mathrm{j}\phi_d}+\mathrm{e}^{-\mathrm{j}\phi_d}\right)U_1U_2\right] = 0, \quad (23a)$$

$$\omega_{d2} + \frac{3\kappa}{8m}\left[\left(2+\mathrm{e}^{-\mathrm{j}2\phi_d}\right)U_1^2 + U_2^2 - U_1^3U_2^{-1}\mathrm{e}^{-\mathrm{j}\phi_d} - \left(2\mathrm{e}^{-\mathrm{j}\phi_d}+\mathrm{e}^{+\mathrm{j}\phi_d}\right)U_1U_2\right] = 0, \quad (23b)$$

where we have used

$$\omega_{d1} = \omega_{n1}^2 - \Omega^2, \quad \text{and} \quad \omega_{d2} = \omega_{n2}^2 - \Omega^2. \quad (24)$$

Taking the imaginary parts of Eqs. (23) leads to

$$U_2^2\sin(2\phi_d) - U_1U_2\sin(\phi_d) - U_1^{-1}U_2^3\sin(\phi_d) = 0, \quad (25a)$$

$$U_1^2\sin(2\phi_d) - U_1U_2\sin(\phi_d) - U_1^3U_2^{-1}\sin(\phi_d) = 0, \quad (25b)$$

which may be satisfied by either

$$\sin(\phi_d) = \sin(\phi_1 - \phi_2) = 0, \quad (26a)$$

$$\text{or} \quad \cos(\phi_d) = \cos(\phi_1 - \phi_2) = \frac{U_1^4 - U_2^4}{2U_1U_2(U_1^2 - U_2^2)}. \quad (26b)$$

Taking the real parts of Eqs. (23) leads to

$$\omega_{d1} + \frac{3\kappa}{8m}\left[U_1^2 + (\cos(2\phi_d)+2)U_2^2 - \left(3U_1U_2 + U_1^{-1}U_2^3\right)\cos(\phi_d)\right] = 0, \quad (27a)$$

$$\omega_{d2} + \frac{3\kappa}{8m}\left[U_2^2 + (\cos(2\phi_d)+2)U_1^2 - \left(3U_1U_2 + U_1^3U_2^{-1}\right)\cos(\phi_d)\right] = 0. \quad (27b)$$

From this it can be found that the phase relationship described by Eq. (26b) cannot be satisfied. Hence, from Eq. (26a), the phase difference between u_1 and u_2 on the backbone curves is

$$|\phi_d| = |\phi_1 - \phi_2| = 0, \pi. \quad (28)$$

We now define $p = \cos(\phi_d)$ where $p = +1$ describes backbone curves where $|\phi_d| = 0$, and $p = -1$ describes backbone curves where $|\phi_d| = \pi$. This allows Eqs. (27) to be written

$$\omega_{d1}U_1 + \frac{3\kappa}{8m}[U_1 - pU_2]^3 = 0, \quad (29a)$$

$$\omega_{d2}U_2 - p\frac{3\kappa}{8m}[U_1 - pU_2]^3 = 0, \quad (29b)$$

which leads to the relationship between U_1 and U_2

$$U_1 = -p\frac{\omega_{d2}}{\omega_{d1}}U_2. \quad (30)$$

Recalling Eqs. (24), and using the restriction that both U_1 and U_2 must be real and positive, we can conclude that $p = +1$ when $\omega_{n1} < \Omega < \omega_{n2}$ and $p = -1$ in all other cases. Next, substituting Eq. (30) into Eq. (29a) leads to

$$\omega_{d2} + \frac{3\kappa}{8m}\left[\frac{\omega_{d2}}{\omega_{d1}} + 1\right]^3 U_2^2 = 0, \quad (31)$$

hence U_2 may be determined using

$$U_2^2 = \frac{-8m\omega_{d2}}{3\kappa}\left(\frac{\omega_{d1}}{\omega_{d1}+\omega_{d2}}\right)^3, \quad (32)$$

showing that U_2 is independent of p. For U_2 to be real, and assuming $\kappa > 0$, we require

$$\omega_{d2}\left(\frac{\omega_{d1}}{\omega_{d1}+\omega_{d2}}\right)^3 < 0. \quad (33)$$

There are three cases to consider. Firstly when $\Omega > \omega_{n2}$, $\omega_{d1} < 0$ and $\omega_{d2} < 0$, applying Eq. (33) leads to

$$\frac{\omega_{d1}}{\omega_{d1}+\omega_{d2}} > 0, \quad (34)$$

which is satisfied. Hence, a valid solution is possible.

When $\Omega < \omega_{n1}$, $\omega_{d1} > 0$ and $\omega_{d2} > 0$, applying Eq. (33) gives

$$\frac{\omega_{d1}}{\omega_{d1} + \omega_{d2}} < 0, \tag{35}$$

which cannot be satisfied.

When $\omega_{n1} < \Omega < \omega_{n2}$, $\omega_{d1} < 0$ and $\omega_{d2} > 0$, applying Eq. (33) leads to

$$\frac{\omega_{d1}}{\omega_{d1} + \omega_{d2}} < 0, \tag{36}$$

which requires that $\omega_{d1} + \omega_{d2} > 0$. Substituting Eqs. (24) and rearranging gives the inequality

$$\Omega < \sqrt{1/2\left(\omega_{n1}^2 + \omega_{n2}^2\right)}. \tag{37}$$

Hence, backbone curves only exist when $\omega_{n1} < \Omega < \sqrt{1/2\left(\omega_{n1}^2 + \omega_{n2}^2\right)}$ and $\Omega > \omega_{n2}$.

If the harmonic content of the response is small (i.e. $\mathbf{h}$ is small) then we may make the approximation $\mathbf{q} \approx \mathbf{u}$ (see Section 2.3). Using the relationships $x_1 = q_1 + q_2$ and $x_2 = q_1 - q_2$ determined from the linear modal transform (see Section 2.2) we can then make the approximations $x_1 \approx u_1 + u_2$ and $x_2 \approx u_1 - u_2$. As u_1 and u_2 are both responding at frequency Ω: $X_1 \approx U_1 + U_2$ and $X_2 \approx |U_1 - U_2|$ when u_1 and u_2 are in-phase (i.e. $p = +1$); $X_1 \approx |U_1 - U_2|$ and $X_2 \approx U_1 + U_2$ when u_1 and u_2 are anti-phase (i.e. $p = -1$). Using Eq. (30), these can be written:

$$p = +1: \quad X_1 \approx \left(1 - \frac{\omega_{d2}}{\omega_{d1}}\right) U_2, \quad X_2 \approx \left|1 + \frac{\omega_{d2}}{\omega_{d1}}\right| U_2, \tag{38a}$$

$$p = -1: \quad X_1 \approx \left|1 - \frac{\omega_{d2}}{\omega_{d1}}\right| U_2, \quad X_2 \approx \left(1 + \frac{\omega_{d2}}{\omega_{d1}}\right) U_2. \tag{38b}$$

Therefore the physical coordinate amplitudes may be written

$$X_1 \approx \left|1 - \frac{\omega_{d2}}{\omega_{d1}}\right| U_2, \qquad X_2 \approx \left|1 + \frac{\omega_{d2}}{\omega_{d1}}\right| U_2, \tag{39}$$

regardless of the value of p. Combining this with Eqs. (24) and (32), leads to

$$X_1 = \left|\frac{\omega_{n1}^2 - \omega_{n2}^2}{\omega_{n1}^2 - \Omega^2}\right| U_2, \qquad X_2 = \left|\frac{\omega_{n1}^2 + \omega_{n2}^2 - 2\Omega^2}{\omega_{n1}^2 - \Omega^2}\right| U_2, \tag{40a}$$

$$\text{where} \quad U_2 = \sqrt{\frac{8m\left(\Omega^2 - \omega_{n2}^2\right)}{3\kappa}\left(\frac{\omega_{n1}^2 - \Omega^2}{\omega_{n1}^2 + \omega_{n2}^2 - 2\Omega^2}\right)^3}. \tag{40b}$$

From this we can calculate the backbone curves in the projection of the response frequency, Ω, against the physical coordinates, X_1 and X_2, as shown in Figure 2. The backbone curves originating at $\Omega = 1$ and $\Omega = 1.1$ are labelled *S1* and *S2* respectively. It can be seen that *S1* tends asymptotically to $\Omega = \sqrt{1/2\left(\omega_{n1}^2 + \omega_{n2}^2\right)} \approx 1.0512$, and that no backbone curve exists between $1.0512 < \Omega < 1.1$, as predicted.

The backbone curves of a system are representative of its underlying behaviour, and the forced response of the system will tend to envelope them. This allows conclusions regarding the forced response of the system to be drawn from the backbone curves. It is found that *S1* has a composition dominated by the first linear mode, q_1. As this system is forced purely in q_2 – see Eq. (15) – we can conclude that this forced response has only a weak tendency to envelope this backbone curve. Meanwhile *S2* is composed primarily of q_2, making the forced response strongly attracted to it. *S2* shows the properties of a response that is well suited for use as a vibration absorber or energy harvester, as the response amplitude of the first mass, X_1, is held at a low value across a large bandwidth, whilst X_2 the response is high, showing that most of the energy is held in the second mass. Although the response of X_1 is high in *S1*, the weak attraction of the forced response to this backbone curve means that this high amplitude should be avoided.

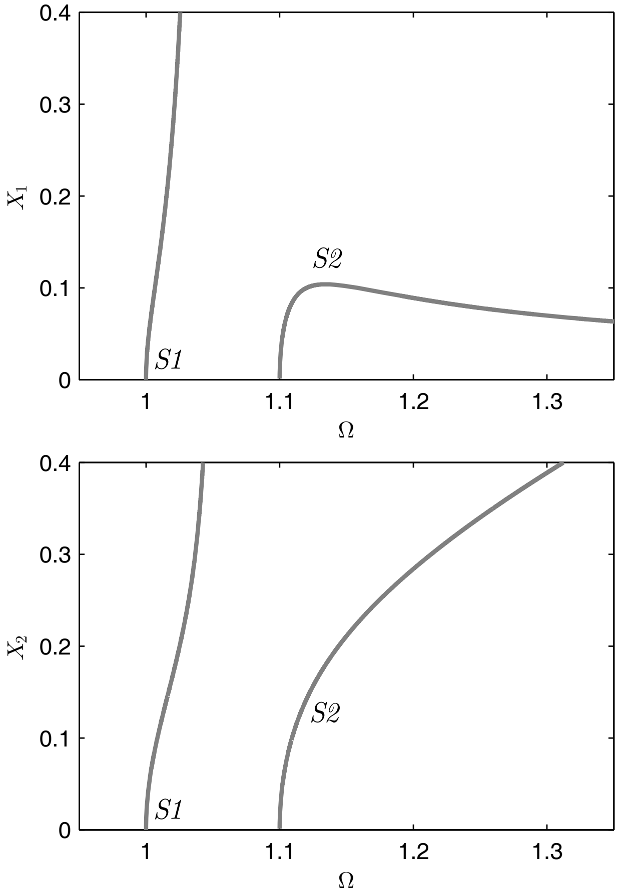

Figure 2. Backbone curves of the system when $\kappa = 5$ in the projection of response frequency, Ω, against displacement amplitude of the first and second mass, X_1 and X_2, in panels (a) and (b) respectively.

4 ENERGY BALANCING

Backbone curves describe the underlying behaviour of a system, however they cannot be used directly to determine which specific behaviours will be seen when a particular forcing and damping are applied. Energy balancing allows these behaviours to be determined, providing a method of relating backbone curves to specific forced responses. It is based on the concept of the *boundary* of a system, over which energy may only cross due to the forcing and damping. For a steady-state response, the net energy crossing the boundary of a system must be zero over one period of motion. Hence the total energy transfer, due to the forcing and damping terms in the equation of motion of the system, must be zero over one period. This must be true for all steady-state solutions in the forced response; however it requires trial solutions that are compatible with the remaining terms. Making the assumption that the forced response crosses the backbone curves, the backbone curves provide a set of trial solutions meeting this requirement. Therefore any points on the backbone curves that satisfy this energy balancing requirement must also represent a point crossed by the forced response.

For the system considered in Section 3, projected onto the linear modes $\mathbf{q}$ – see Eqs. (14) and (15), the terms that may transfer energy over the boundary can be written

$$\begin{pmatrix} D_1\dot{q}_1 \\ D_2\dot{q}_2 - P_2\cos(\Omega t) \end{pmatrix}, \tag{41}$$

where $D_1 = 0.005$, $D_2 = 0.015$ and $P_2 = 0.005$. Each of these terms is representative of a time-varying force acting on the motion of the corresponding mode. Hence, allowing term m for mode n to be written $f_{n,m}(t)$, then the power transferred at time t can be written $f_{n,m}(t)\dot{q}_n$. Therefore, the net energy transferred by this term over one period, $t \in [0,T]$, can be written

$$E_{n,m} = \int_0^T f_{n,m}(t)\dot{q}_n \mathrm{d}t, \tag{42a}$$

$$\approx -U_n\Omega \int_0^T f_{n,m}(t)\sin(\Omega t - \phi_n)\mathrm{d}t. \tag{42b}$$

The terms in the form $D_n\dot{q}_n$ can be approximated to

$$D_n\dot{q}_n \approx -D_nU_n\Omega\sin(\Omega t - \phi_n), \tag{43}$$

which may be substituted into Eq. (42b) to give

$$E_{n,m} = D_nU_n^2\Omega^2 \int_0^T \sin^2(\Omega t - \phi_n)\mathrm{d}t, \tag{44a}$$

$$= \frac{1}{2}D_nU_n^2\Omega^2\left[t - \frac{\sin(2\Omega t - 2\phi_n)}{2\Omega}\right]_{t=0}^{t=T}, \tag{44b}$$

$$= \pi D_nU_n^2\Omega, \tag{44c}$$

where $T = 2\pi/\Omega$ has been used. For the remaining term, the energy may be calculated as

$$E_{n,m} = P_2U_2\Omega \int_0^T \cos(\Omega t)\sin(\Omega t - \phi_2)\mathrm{d}t, \tag{45a}$$

$$= \frac{1}{2}P_2U_2\Omega\left[t\sin(\phi_2) - \frac{\cos(2\Omega t - \phi_2)}{2\Omega}\right]_{t=0}^{t=T}, \tag{45b}$$

$$= \pi P_2U_2\sin(\phi_2). \tag{45c}$$

Therefore, the net energy crossing the system boundary is

$$\pi D_1U_1^2\Omega + \pi D_2U_2^2\Omega + \pi P_2U_2\sin(\phi_2) = 0. \tag{46}$$

when in steady-state. On the backbone curves, the inertia of all components of the two modes are balanced. Hence, for the response of the forced system to cross the backbone curve, the forcing must balance with the damping without interfering with other components. As the damping is acting on the velocity component of the motion, it is always at an angle $-\pi/2$ behind the displacement. Hence, to balance this, the forcing must be $+\pi/2$ ahead of the displacement, i.e. $\phi_2 = -\pi/2$. Therefore, we can write

$$(D_1U_1^2 + D_2U_2^2)\Omega = P_2U_2. \tag{47}$$

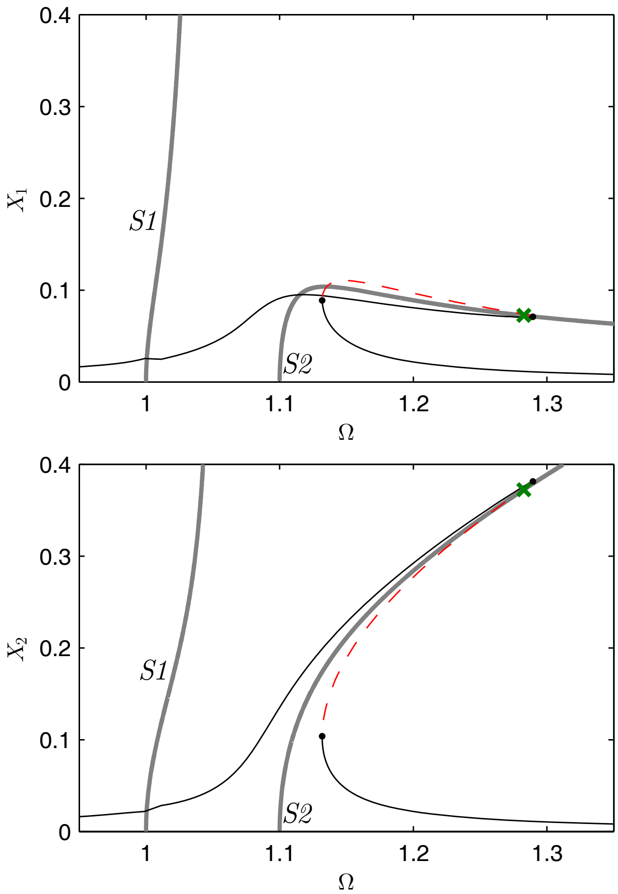

Figure 3. Backbone curves and forced response of the system when $\kappa = 5$ in the projection of response frequency, Ω, against displacement amplitude of the first and second mass, X_1 and X_2, in panels (a) and (b) respectively. Thick grey lines represent the backbone curves and the forced response is shown as thin black lines and dashed red lines for the stable and unstable branches respectively. Green crosses represent the crossing points predicted by energy balancing and the fold points on the forced response are represented by black dots.

Figure 3 shows the energy balancing technique applied to the example system, with the parameters given in Eq. (12) where $\kappa = 5$. The backbone curves and the crossing points predicted by the energy balancing technique are compared to the forced response. It can be seen that, as expected, the forced response does not tend towards *S1*, due to the low q_2 component in *S1*. Hence, no crossing point has been predicted here. The predicted crossing point on *S2* is good, although not precise. This is due to the fact that on the backbone curves, there is no net energy transfer between q_1 and q_2. However, as q_1 is damped but unforced, the forced response must be such that there is a net energy flow from q_2 to q_1. Therefore, the assumption that the forced response crosses the backbone curves precisely cannot be true.

5 OPTIMISATION

As an example of how the technique may be used to optimise a system, consider the case where an energy harvesting device connects the second mass to ground. As this device acts like a damper, it does not affect the backbone curves but does affect the point at which the forced response crosses the backbone curves, as predicted by the energy balancing technique. Therefore, by varying the nonlinear parameter, κ, we can describe the change in the underlying behaviour using the backbone curves and the change in the forced response using the energy balancing technique. This approach can be used to optimise the system with respect to κ.

For this example, it is required that the maximum displacement of the first mass, X_1, must not exceed 0.125, whilst it is desirable to maximise the potential of the system to harvest energy. As the basin of attraction of the upper branch decreases with Ω, we estimate the probability that the response will settle to the upper branch of the response, as

$$P(\Omega) = \frac{\Omega_{EB} - \Omega}{(\Omega_{EB} - \omega_{n2})\left[1000\,(\Omega - \omega_{n2})^2 + 1\right]}, \quad (48)$$

where Ω_{EB} is the value of Ω at the crossing point determined by the energy balancing.

5.1 *FINDING THE MAXIMUM VALUE OF X_1*

From Figure 2 it can be seen that the maximum value of X_1 occurs at the point where $\frac{dX_1}{d\Omega} = 0$. From Eqs. (40), this can be found using

$$\frac{d}{d\Omega}\left[\frac{\omega_{n2}^2 - \omega_{n1}^2}{\Omega^2 - \omega_{n1}^2} U_2(\Omega)\right] = 0, \quad (49a)$$

$$\frac{-2\Omega\left(\omega_{n2}^2 - \omega_{n1}^2\right)}{\left(\Omega^2 - \omega_{n1}^2\right)^2} U_2(\Omega) + \frac{\omega_{n2}^2 - \omega_{n1}^2}{\Omega^2 - \omega_{n1}^2} U_2'(\Omega) = 0, \quad (49b)$$

$$\frac{2\Omega}{\omega_{d1}} U_2(\Omega) + U_2'(\Omega) = 0, \quad (49c)$$

where $\bullet'$ represents $\frac{d\bullet}{d\Omega}$ and, from Eq. (32)

$$U_2(\Omega) = \left(\frac{8m\left(\Omega^2 - \omega_{n2}^2\right)}{3\kappa}\right)^{\frac{1}{2}} \left(\frac{\omega_{n1}^2 - \Omega^2}{\omega_{n1}^2 + \omega_{n2}^2 - 2\Omega^2}\right)^{\frac{3}{2}}, \quad (50a)$$

$$= (A)^{\frac{1}{2}} (B)^{\frac{3}{2}}, \quad (50b)$$

where

$$A = \frac{-8m\omega_{d2}}{3\kappa}, \qquad B = \frac{\omega_{d1}}{\omega_{d1} + \omega_{d2}}. \quad (51)$$

From this, we can calculate

$$U_2'(\Omega) = A^{\frac{1}{2}} \frac{d}{d\Omega}\left[B^{\frac{3}{2}}\right] + B^{\frac{3}{2}} \frac{d}{d\Omega}\left[A^{\frac{1}{2}}\right], \quad (52a)$$

$$= \frac{3}{2} A^{\frac{1}{2}} B^{\frac{1}{2}} B' + \frac{1}{2} A^{-\frac{1}{2}} B^{\frac{3}{2}} A', \quad (52b)$$

where

$$A' = \frac{d}{d\Omega}\left[\frac{8m\left(\Omega^2 - \omega_{n2}^2\right)}{3\kappa}\right], \quad (53a)$$

$$= \frac{16m\Omega}{3\kappa}, \quad (53b)$$

and

$$B' = \frac{d}{d\Omega}\left[\frac{\omega_{n1}^2 - \Omega^2}{\omega_{n1}^2 + \omega_{n2}^2 - 2\Omega^2}\right], \quad (53c)$$

$$= \frac{2\Omega\,(\omega_{d1} - \omega_{d2})}{(\omega_{d1} + \omega_{d2})^2}. \quad (53d)$$

Substituting Eqs. (53b) and (53d) into Eq. (52b) leads to

$$U_2' = (AB)^{\frac{1}{2}} \left(\frac{3\Omega\,(\omega_{d1} - \omega_{d2})}{(\omega_{d1} + \omega_{d2})^2}\right) + \frac{B^{\frac{3}{2}}}{A^{\frac{1}{2}}} \left(\frac{8m\Omega}{3\kappa}\right). \quad (54)$$

Substituting Eqs. (50b) and (54) into Eq. (49c) and simplifying gives

$$\omega_{d1}^2 + \omega_{d2}^2 - 4\omega_{d1}\omega_{d2} = 0. \quad (55)$$

This can then be written as a quadratic in Ω^2, using Eq. (24), and solved to give

$$2\Omega^2 = \omega_{n1}^2 + \omega_{n2}^2 \pm \sqrt{3}\left(\omega_{n2}^2 - \omega_{n1}^2\right). \quad (56)$$

As Ω must be real, the positive root must be chosen, leading to

$$\Omega = \sqrt{\left(\frac{1-\sqrt{3}}{2}\right)\omega_{n1}^2 + \left(\frac{1+\sqrt{3}}{2}\right)\omega_{n2}^2}, \quad (57)$$

which shows that the frequency at which the maximum value of X_1 occurs is independent of κ. Substituting this into Eqs. (39), (32) and (24) it is found that the maximum value of X_1 on the backbone curve is given by

$$X_{1,MAX} = \sqrt{\frac{4\sqrt{3}\left(\omega_{n2}^2 - \omega_{n1}^2\right) m}{27\kappa}}. \quad (58)$$

For X_1 to be less than 0.125, it is required

$$\kappa > \frac{4\sqrt{3}\left(\omega_{n2}^2 - \omega_{n1}^2\right) m}{27(0.125)^2}, \quad (59a)$$

$$> 3.45 \qquad \text{(to 3 significant figures).} \quad (59b)$$

5.2 *OPTIMISING FOR X_2*

With a minimum value for κ defined by Eqs. (59) we can now optimise the system with respect to its potential to harvest energy. The energy harvested from the device is proportional to the velocity of x_2, i.e. proportional to ΩX_2. Using Eq. (48), we can define the probabilistic energy harvesting capability at a given Ω (where $\Omega \in [\omega_{n2}, \Omega_{EB}]$) as $P(\Omega)\Omega X_2$. Therefore, the overall capability of the system in harvesting energy over all forcing frequencies is given by the proportional relation

$$E_H \propto \int_{\omega_{n2}}^{\Omega_{EB}} P(\Omega)\Omega X_2 d\Omega, \quad (60)$$

where Ω_{EB} can be found from Eq. (46).

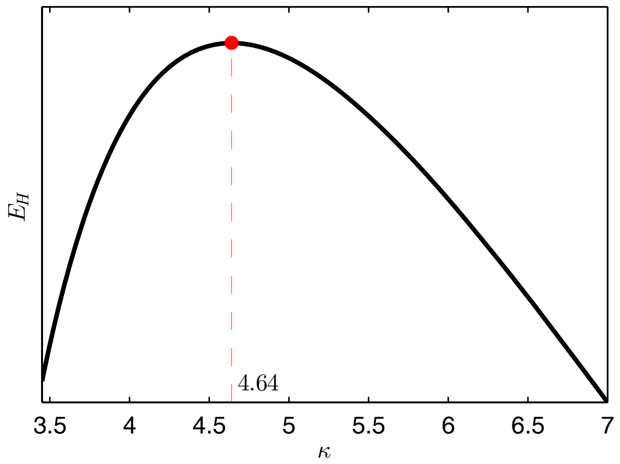

Figure 4. Nonlinear coefficient, κ, against proportional energy harvesting capability of the system. The red dot shows the point at which the energy harvesting capability is at its maximum.

This may be calculated for a range of values of κ, where $\kappa > 3.45$ in keeping with Eq. (59b). Figure 4 shows κ against proportional energy harvesting capability of the system. The point of maximum capability is represented by a red dot, and corresponds to $\kappa = 4.64$. At this value the maximum value of X_1 is given by $X_1 = 0.1078$, which is below the limit of 0.125.

6 CONCLUSION

This work shows how the second-order normal form technique can be used to develop analytical expressions describing the response of MDOF nonlinear systems. We have demonstrated that by describing the backbone curves of such systems we can interpret the underlying behaviour, independent of forcing and damping. This provides a simple method for determining the characteristics of nonlinear systems, and is well suited for use in the analysis of larger systems. Backbone curves also allow some features of the response of a system to be optimised independently of forcing and damping. This provides a simplification of the response along with a design tool for nonlinear systems where the forcing and damping characteristics are unknown.

The relationship between backbone curves and the forced response can be determined using the energy balancing technique introduced here. This may allow further simplification of systems by disregarding backbone curves that are not followed under particular forcing and damping conditions. As the energy balancing technique is also analytical, it may be used alongside the analytical design and optimisation enabled by the second-order normal form technique. The accuracy may be further increased by accounting for the harmonic terms in both the backbone curves and the energy balancing technique, and by allowing for a higher order of accuracy in the second-order normal form technique.

The limitations of this approach are dictated by the need for the systems to be weakly nonlinear, in order for the second-order normal form technique to be valid. It is preferable that, when the system is forced, the energy transfer within the system is small. This allows the forced response to approach the backbone curves, increasing the accuracy of the energy balancing technique.

REFERENCES

[1] E.J. Doedel, with major contributions from A.R. Champneys, T.F. Fairgrieve, Y.A. Kuznetsov, F. Dercole, B.E. Oldeman, R.C. Paffenroth, B. Sandstede, X.J. Wang and C. Zhang, *AUTO-07P: Continuation and Bifurcation Software for Ordinary Differential Equations*, Concordia University, Montreal, Canada, (2008). http://cmvl.cs.concordia.ca .

[2] G. Kerschen, M. Peeters, J.C. Golinval and A.F. Vakakis, Nonlinear normal modes, Part I: A useful framework for the structural dynamicist, *Mechanical Systems and Signal Processing*, 23, 170 - 194, (2009).

[3] M. Peeters, R. Vigui, G. Srandour, G. Kerschen and J.C. Golinval, Nonlinear normal modes, Part II: Toward a practical computation using numerical continuation techniques, *Mechanical Systems and Signal Processing*, 23, 195 - 216, (2009).

[4] A.H. Nayfeh and D.T. Mook, *Nonlinear Oscillations*, Wiley, (2008).

[5] R. Khanin, M. Cartmell and A, Gilbert, A computerised implementation of the multiple scales perturbation method using Mathematica, *Computers & Structures*, 76, 565-575, (2000).

[6] D.I.M. Forehand and M.P. Cartmell, The implementation of an automated method for solution term-tracking as a basis for symbolic computational dynamics, *Proceedings of the Institution of Mechanical Engineers, Part C: Journal of Mechanical Engineering Science*, 225, 40-49, (2011).

[7] J. Murdock, *Normal Forms and Unfoldings for Local Dynamical Systems*, Springer, (2002).

[8] S.A. Neild, Approximate Methods for Analysing Nonlinear Structures, *Exploiting Nonlinear Behavior in Structural Dynamics*, Springer, Vienna, CISM Courses and Lectures, 53-109, (2012).

[9] S.A. Neild and D.J. Wagg, Applying the method of normal forms to second-order nonlinear vibration problems, *Proceedings of the Royal Society A: Mathematical, Physical and Engineering Science*, 467, 1141-1163, (2010).

[10] D.J. Wagg and S.A. Neild, *Nonlinear Vibration with control*, Springer-Verlag, (2009).